

**Pharmacological modulation of right ventricular endocardial-epicardial gradients
in Brugada Syndrome**

**J. Bhar-Amato*, M. Finlay*, D. Santos, M. Orini, V. Vyas, P. Taggart, A. A. Grace, C. L.-
H. Huang, R. Ben-Simon, A. Tinker, P. D. Lambiase**

Total Word Count 4699

Subject Headings: autonomic nervous system, electrophysiology, sudden cardiac death

***Joint first authorship**

Addresses for Correspondence:

**PD Lambiase
UCL Institute of Cardiovascular Science & Barts Heart Centre
Room 3.20
Rayne Institute,
5 University Street
London WC1E 6JF**

Acknowledgements:

JBA was funded by a *Heart Research UK Fellowship*.
MO is funded by a Marie Curie Fellowship.
DS funded by an MRC CASE Studentship
PDL is supported by UCLH Biomedicine NIHR & Stephen Lyness Memorial Fund.
CLHH funded by the British Heart Foundation.

Conflicts of interest: None.

ABSTRACT

Background

We explored the hypothesis that increased cholinergic tone exerts its pro-arrhythmic effects in Brugada Syndrome (BrS) through increasing dispersion of transmural repolarisation in patients with spontaneous and drug induced Brugada Syndrome.

Methods & Results

Electrophysiological studies in control patients with SVT only demonstrated shorter endocardial than epicardial right ventricular (RV) activation times (AT's) (mean difference: 26 ms, $p<0.001$). In contrast, BrS patients showed longer endocardial than epicardial AT (mean difference: -15 ms, $p=0.001$). BrS hearts, compared to controls, showed significantly larger transmural gradients (TMG) in their activation recovery intervals (ARIs) (mean intervals 20.5 vs 3.5 ms; $p<0.01$), with longer endocardial than epicardial ARIs. Edrophonium challenge increased such gradients in both controls (to a mean of 16 msec ($p<0.001$)) and BrS (to 29.7 ms; $p<0.001$). However, these were attributable to *epicardial* and *endocardial* ARI prolongations in control and BrS hearts respectively. Dynamic changes in repolarisation gradients were also observed across the BrS RV wall in BrS.

Conclusions:

Differential contributions of conduction and repolarisation were identified in BrS which critically modulated transmural dispersion of repolarisation with significant cholinergic effects only identified in the BrS patients. This has important implications for explaining the pro-arrhythmic effects of increased vagal tone in BrS as well as evaluating autonomic modulation & epicardial ablation as therapeutic strategies.

Key Words: Brugada Syndrome, Autonomic nervous system, Conduction, Repolarisation

INTRODUCTION

Brugada Syndrome (BrS) remains one of the most important causes of sudden cardiac death in the young, accounting for 20% of such cases¹. Its molecular basis remains uncertain. Ion channel mutations primarily involving the sodium channel have only been identified in up to 30% of subjects². The pathophysiological basis for its associated arrhythmias also remains contentious. BrS is characterised by a triad of right bundle branch block (RBBB), coved ST elevation in the right precordial leads and lethal ventricular arrhythmias. The disease appears localised to the right ventricle (RV) where dynamic changes in ST elevation and ventricular arrhythmias develop in situations of increased vagal tone.

High density intra-cardiac mapping by our group has identified significant conduction delays in the RV outflow tract (RVOT) compared to the RV body and apex in BrS relative to findings in control patients³. These data have been corroborated and it is now evident that BrS is further associated with marked epicardial conduction abnormalities and increased fibrosis⁴⁻⁷. Such fibrotic changes could lead to electrotonic uncoupling between myocytes with source:sink mismatches between endocardium and epicardium. These could produce the alterations in conduction or repolarisation gradients reported in a recent mechanistic human study⁸. BrS has a more common nocturnal occurrence of ventricular fibrillation which occurs in parallel with a corresponding nocturnal accentuation of its pathognomonic ECG features⁹. These in turn correspond to the increased vagal and diminished sympathetic activity during periods of rest¹⁰. However, the electrophysiological effects of changes in autonomic tone on the BrS substrate remain uncertain.

100 Here we explore the hypothesis that in BrS such increased cholinergic tone induces
101 conduction delay and promotes either intramural or transmural dispersions of
102 repolarisation in the RVOT. We evaluated the effect of cholinergic activation on in vivo
103 electrophysiological properties of the RV endocardium and RV epicardium in BrS
104 patients.

105

106

METHODS

The data, analytic methods, and study materials will be made available to other researchers for purposes of reproducing the results or replicating the procedure on direct request.

Human electrophysiological mapping

The non-contact mapping study and pacing protocol were performed prior to ablation in the control patients or VT stimulation studies in the Brugada Syndrome (BrS) group. All anti-arrhythmic drugs had first been stopped for at least 5 half lives prior to the procedures. The detailed techniques for non-contact mapping in the ventricle are described elsewhere¹². The multi-electrode array (MEA) (*Ensite*, St Jude Medical, St. Paul, Minnesota, USA) was deployed via the left femoral vein in the right ventricular outflow tract (RVOT) (full methodology described previously³). An epicardial 16-pole Pathfinder catheter (Cardima, California, USA) was passed into the distal great cardiac vein in the interventricular groove (Fig. 1). All patients gave informed consent and the study was approved by the University College London Hospital (UCLH) Research Ethics Committee.

Programmed ventricular stimulation was performed from the right ventricular apex. Three minutes of steady state pacing at a coupling interval of 400 ms was followed by a S₁S₂ restitution protocol using 400 ms drive trains. The extrastimulus was initially extended progressively by 50 ms intervals until consistent fusion with sinus beats occurred. The S₁S₂ interval was thereafter decreased at 20 ms intervals to 300 ms, then by 5 ms until the ventricular effective refractory period (VERP) was reached. The protocol was repeated following intravenous (IV) administration of 10 mg edrophonium to increase cholinergic tone, then followed by a 10 min washout period.

Offline analysis

24 virtual unipolar electrograms were placed in the RVOT in 4 columns of 6 virtuals to obtain local endocardial data within 3 cm of the array directly opposite the position of the 16 pole Cardima catheter (Fig. 1). Endocardial & epicardial electrograms were exported and analysed using semi-automated custom software running in Matlab (The Mathworks Inc., MA, USA) (Figure S1). All electrograms and analyses were manually checked by 3 independent observers (JBA, MF, DS). The time from the earliest electrogram recorded within the right ventricle (RV) to the steepest negative deflection ($(dV/dt)_{\min}$) was used as the local activation time (AT). The sinus rhythm AT of the RV was taken as the time from earliest to latest recorded RV activation. During pacing, the time from the pacing artefact to the time corresponding to the $(dV/dt)_{\min}$ was used as the local AT. Two methods have been used to measure repolarisation times during non-contact mapping, respectively termed the classical (Wyatt) method and the alternative method. Both have come under intense theoretical and experimental scrutiny; here we present results using the classical method¹³⁻¹⁶. Activation repolarisation interval (ARI), a well-validated approximation of action potential duration, was defined as the interval between the AT and repolarization time (Figure S1). The slope of ARI restitution was calculated using the least mean squares method^{17,18}. The RVOT was divided into 4 anatomical regions (anterior, posterior, lateral septal), and activation and repolarisation dynamics were studied in the RVOT endocardium and epicardium.

Endocardial & Epicardial Regional Delay

Mean increase of delay (MID) was calculated by dividing the integrated increase of delay (area under the curve) by the interval between baseline cycle length and the refractory period.¹⁹ The degree of delay was measured from 4 segments in the RVOT and in the epicardium.

Genetic testing

Blood samples (10 mL) were obtained from participating BS subjects. Genomic DNA was isolated from peripheral blood leukocytes with the use of a commercial kit (Gentra System, Puregene). The exons of SCN5A were amplified and analyzed by direct sequencing. Polymerase chain reaction products were purified with Exosap (USB) and were directly sequenced from both directions with the ABI PRISM BigDye Terminator Cycle Sequencing Reaction and the ABI PRISM 3130XL Automatic DNA Sequencer.

Statistical analysis

All statistical computing was performed using R software (The Comprehensive R Archive Network (CRAN)). Continuous parametric data are presented as means \pm standard deviations (SD) or, in the case of significance derived from regression models, mean with [95% confidence interval], unless otherwise specified. Comparisons in which a single measurement was taken for each subject, e.g. ventricular effective refractory period (VERP), dispersion of repolarisation time, were made using Student's t-test with post-hoc correction for multiple comparisons. Continuous parametric data derived from electrogram data were modelled using mixed-effects linear regression (software: Linear and Nonlinear Mixed Effects (NLME) package running in R version 2.14) and statistical significance was inferred from the model. Quartile regression with bootstrapping (Quantile Regression Description Estimation and inference (QUANTREG) package) was used to compare non-parametric continuous data.

RESULTS

Mapping was performed in 16 patients (BrS group: n = 8, 5M: 2F; mean age 56 y, control group: n=8, 5M: 3F; mean age 48,). The demographic data is shown in Table 1. Four BrS patients had resting type 1 ECGs and two had a family history of sudden cardiac death. No significant structural abnormalities were detected on echocardiography or MRI with MRI excluding gadolinium late enhancement or T1 mapping abnormalities in the right

and left ventricles in the 4 scanned cases. Only one patient had an ICD inserted for symptomatic non-sustained VT and none have had any significant ventricular arrhythmic events in 8 years of follow-up.

Genetic data are available in 4 subjects: BrS cases 3-5 were negative for known pathogenic SCN5A mutations and BrS subject 8 was a carrier of a c.3045_3046delGA, exon 17 SCN5A, which is predicted to cause a frameshift of the amino acid sequence in leading to a premature termination of translation.

Formatted: Font color: Red

The control group of patients had SVT. They had normal resting and signal averaged ECGs, a negative ajmaline challenge test, structurally normal hearts on echocardiography and no family history of sudden cardiac death. Informed consent was obtained following local research ethics committee approval. We used the acetylcholinesterase inhibitor edrophonium to activate muscarinic receptors.

We made direct measurements of epicardial and endocardial activation times (AT), and activation recovery intervals (ARI), from which we further derived recovery times (RTs) in both control and BrS patients before and following autonomic edrophonium challenge. This permitted us to derive the transmural gradients in AT, ARI and RTs, relating these phenotypic characteristics to findings in BrS or normal patients.

During *steady pacing*, epicardial *activation times* (ATs) and *activation recovery intervals* (ARIs) were significantly shorter in BrS than in control patients and neither were significantly affected by edrophonium challenge (Fig. S2). In contrast, endocardial AT and ARI were significantly longer in BrS than control patients, and similarly only minimally affected by edrophonium challenge.

Measurements made through *varying coupling intervals used to construct restitution curves* demonstrated that control patients showed shorter endocardial than epicardial ATs that gave mean AT differences of 26 ms, 95% CI: 21, 32 for endocardium and epicardium respectively, $p < 0.001$ (Fig. 2). In contrast, the BrS patients showed longer endocardial AT than epicardial AT (mean AT difference: 15 ms, 95% CI 11, 20, for endocardium and epicardium respectively; $p = 0.001$). Following edrophonium challenge, both endocardial and epicardial ATs were unchanged in the control but significantly further shortened in the BrS patients. However, neither control nor BrS patients showed significant changes in their transmural activation time differences. When we measured the regional delay to assess conduction reserve, this was greater in the epicardium than endocardium in BrS versus controls and was further exaggerated following edrophonium (Fig S3).

Hearts from the control patients showed minimal transmural gradients (TMG) in their ARIs (mean 3.4 ms, 95% CI: 6.8, 0.02, $p < 0.05$) with endocardial ARIs that were marginally shorter than epicardial ARIs (Fig. 3). In contrast, hearts from the BrS patients showed significantly larger TMG (mean 20.5 ms, 95% CI: 25.5, 15.5, $p < 0.001$), with shorter epicardial ARIs than endocardial ARIs.

Following edrophonium challenge, the TMG in hearts from control patients increased to a mean of 16 ms (95% CI: 19.6, 12.6, $p < 0.001$), and this reflected an *epicardial* ARI prolongation. The TMG in hearts from BrS patients increased to 29.7 ms (95% CI: 35.3, 24.1, $p < 0.001$), but this reflected *endocardial* as opposed to epicardial ARI prolongation. These effects were particularly evident from contact endocardial and epicardial electrogram recordings illustrating the unipolar electrogram morphologies in hearts from BrS versus control patients and the effects of edrophonium on the degree of ST elevation in the epicardium (Fig. 4).

In control patients, epicardial repolarisation as reflected in its **repolarisation times (RT)** was completed later than endocardial repolarisation. The resulting RT gradient therefore ran from epi- to endocardium. However, in the BrS patients, epicardial repolarisation was completed earlier than endocardial repolarisation and showed smaller values at long cycle lengths. This resulted in a reversed RT gradient with significantly shorter epicardial versus endocardial RTs. Edrophonium challenge left the RT gradient flat and unaffected across all the coupling intervals in the control patients. In contrast, in the BrS patients, edrophonium challenge resulted in a significant increase in the epicardial RTs which was most pronounced at longer CI's. The RT gradients across the coupling intervals altered particularly at shorter intervals (Fig. 5).

Maximum restitution slopes

Epicardial maximum restitution slopes (S_{max}) at baseline were steeper ($p<0.05$) in hearts of patients with BrS (mean 0.887, SEM 0.065) compared with control patients (mean 0.728, SEM 0.046) with no significant changes following edrophonium challenge. The values of S_{max} in the anterior RVOT endocardium were similar in hearts from BrS and control patients, and showed no significant changes following edrophonium challenge. In contrast, edrophonium decreased the whole RVOT endocardial S_{max} in hearts from control patients (from mean 0.68, SEM 0.031 to mean 0.544, SEM 0.023, $p<0.001$), but produced no significant corresponding changes in hearts from the BrS patients.

Discussion

We report the first detailed *in vivo* investigation of the effects of autonomic modulation on right ventricular endocardial and epicardial electrophysiology in BrS. This revealed

that the modulation of activation and repolarisation gradients by premature stimuli may be greater in BrS.

Our studies determined epicardial and endocardial activation times (AT), activation recovery intervals (ARI), and recovery times (RTs) in both control and BrS patients. From these we derived the corresponding transmural gradients in AT, ARI and RTs before and following autonomic edrophonium challenge and related these phenotypic characteristics to findings in BrS or normal patients. We observed significant effects of both *absolute and transmural differences* between both conduction and repolarisation characteristics and differing effects upon these of cholinergic challenge. We thus associated differences in the spatial organisation and heterogeneity of these changes in activation and repolarisation with the BrS condition.

Our key findings concerned abnormalities in the transmural gradients of both activation and repolarisation in Brugada syndrome patients and their accentuation by cholinergic stimulation. Thus, whereas in control individuals, the epicardium completed repolarisation before the endocardium, in BrS this sequence was reversed. Edrophonium modulated the abnormal transmural gradient in BrS leading to further delayed epicardial repolarisation. This reflected differential effects of the BrS condition and of cholinergic challenge upon conduction velocity and repolarisation which govern the transmural activation sequence. Thus, prior to cholinergic challenge, the main differences between human BrS and controls reflected epicardial differences with the BrS showing shorter ARI's and the epicardium activating earlier than the endocardium. This parallels the findings of other groups^{7,8, 20}. Indeed the largest mean ARI gradient at rest is equivalent: 20.5ms versus 24ms in the Langendorff study of a Brugada heart²⁰. This causes a significant reversed repolarisation gradient to arise from endocardium to epicardium

which did not exist in controls. Increased cholinergic tone through edrophonium administration exerted additional important effects on conduction-repolarisation dynamics in BrS with significant differences in epi and endocardial electrophysiological responses. There is a reversed ARI gradient in BrS patients with shorter epicardial ARI's compared with a smaller opposite ARI gradient in normal individuals at baseline. These differences are exacerbated by increased cholinergic tone with preferential endocardial ARI prolongation in BrS.

The findings may reflect a differential distribution of ion channels between the endocardium and epicardium²¹. Differences in sodium channel, calcium channel and potassium channel expression and differential regulation of currents by autonomic pathways are likely to account for the striking endo and epicardial differences. This indicates a loss of endocardial to epicardial conduction reserve which could be due to abnormalities in the Purkinje network preventing rapid endocardial tissue recruitment and subsequent endo-epicardial depolarisation as well as reduced tissue coupling secondary to lack of Na channel recruitment (excitability) and tissue fibrosis.

The data also show that increased cholinergic tone promotes heterogeneity between epi and endocardium and suggests the main cholinergic effects in BrS are exerted on the endocardial ARI, combined with conduction delays *amplifying transmural repolarisation dynamic differences across coupling intervals*. The marked conduction delays especially at short coupling intervals in these studies in conjunction with the shorter ARI's in the Brugada heart create the optimal conditions to promote large endo-epicardial conduction and repolarisation gradients.

The electrophysiological changes reported here may also bear upon the “conduction and repolarisation hypotheses” explaining the characteristic clinical ECG waveform in BrS²². These variously explain its coved ST elevation by delayed depolarisation from the RV body to RVOT or transmural gradients in repolarisation secondary to a shortened “dip and plateau” action potential morphology in the epicardium. The present findings are consistent with a combination of these mechanisms. This would be compatible with the differential conduction delay between the endocardium and epicardium and the earlier epicardial repolarisation in BrS. Furthermore, changes in coupling interval modulate these features on a beat to beat basis, and this would promote the creation of endocardial-epicardial repolarisation gradients and hence ST elevation in the right precordial leads with the gradients particularly in the presence of electrotonic uncoupling promoted by structural abnormalities^{23,24}.

The findings also have implications for electrocardiographic changes following conditions of increased cholinergic tone in BrS. Thus, increased vagal tone is known to produce dynamic changes in J point elevation and ventricular arrhythmia. Nakazawa et al. reported that high vagal tone and low sympathetic tone are specific properties of symptomatic BrS on the basis of heart rate variability data²⁵. Their study also suggested these autonomic imbalances were significant in the symptomatic group but not in the asymptomatic group. Dynamic changes in J point elevation are more prominent at night particularly in patients with previous VF. Abnormal ¹²³I-MIBG uptake in patients with BrS is described indicating presynaptic sympathetic dysfunction of the heart shifting the influence to increases in cholinergic tone²⁶. The precise relationship between vagal tone and pro-arrhythmia is subject to debate. Increased vagal tone is thought to reduce the Ca transient during phase 2 of the action potential resulting in increased transmural

dispersion of repolarisation and phase 2 re-entry²⁷. The data supporting this hypothesis has been derived from the canine RV wedge preparation of BrS employing pharmacological manipulations to reproduce the Brugada ECG.

This study demonstrates that autonomic effects are 2-fold-promoting endocardial ARI prolongation with marked shortening of endo and epicardial AT. These 2 effects will be highly pro-arrhythmic enabling endocardial functional conduction block and promoting a large vulnerable window epicardially to facilitate re-entry.

Limitations

We were unable to biopsy the sites of recording or undertake direct epicardial recording of the substrate so it is possible that more severely diseased areas were not studied. Nevertheless, these findings indicate sufficient pathology was present to enable significant differences in conduction-repolarisation dynamics to be identified. These findings provide evidence of conduction-repolarisation abnormalities in BrS without events but the extent of such changes need to be explored in more severely affected individuals as there is preliminary evidence to suggest that such cases may have more marked conduction abnormalities using ECG Imaging^{28,29}. Indeed the extent of these changes could be used as a risk marker for lethal arrhythmias.

These data have important clinical implications with recent interest in epicardial substrate ablation to prevent VF in BrS^{30,31}. Ablation appears to normalise the resting ECG and prevent dynamic ST elevation. This may operate by homogenising the substrate such that endo and epicardial gradients can no longer be generated in the RVOT. This will prevent changes in cholinergic tone influencing the gradient & enabling VF initiation if these transmural gradients are primarily responsible for arrhythmogenesis.

References

1. Priori SG, Wilde AA, Horie M, Cho Y, Behr ER, Berul C, Blom N, Brugada J, Chiang CE, Huikuri H, Kannankeril P, Krahn A, Leenhardt A, Moss A, Schwartz PJ, Shimizu W, Tomaselli G, Tracy C; Document Reviewers., Ackerman M, Belhassen B, Estes NA 3rd, Fatkin D, Kalman J, Kaufman E, Kirchhof P, Schulze-Bahr E, Wolpert C, Vohra J, Refaat M, Etheridge SP, Campbell RM, Martin ET, Quek SC; Heart Rhythm Society.; European Heart Rhythm Association.; Asia Pacific Heart Rhythm Society. Executive summary: HRS/EHRA/APHRS expert consensus statement on the diagnosis and management of patients with inherited primary arrhythmia syndromes.. *Europace*. 2013 Oct;15(10):1389-406.
2. [Bezzina CR](#), [Lahrouchi N](#), [Priori SG](#). Genetics of sudden cardiac death, [Circ Res](#). 2015 Jun 5;116(12):1919-36. doi: 10.1161/CIRCRESAHA.116.304030.
3. Lambiase PD, Ahmed AK, Ciaccio EJ, et al. High-density substrate mapping in Brugada syndrome: combined role of conduction and repolarization heterogeneities in arrhythmogenesis. *Circulation* 2009;120:106–17.
4. Postema PG, van Dessel PFHM, de Bakker JMT, et al. Slow and discontinuous conduction conspire in Brugada syndrome: a right ventricular mapping and stimulation study. *Circ Arrhythm Electrophysiol* 2008;1: 379–86.
5. Nademanee K, Raju H, de Noronha SV, Papadakis M, Robinson L, Rothery S, Makita N, Kowase S, Boonmee N, Vitayakritsirikul V, Ratanarapee S, Sharma S, van der Wal AC, Christiansen M, Tan HL, Wilde AA, Nogami A, Sheppard MN, Veerakul G, Behr ER. Fibrosis, Connexin-43, and Conduction Abnormalities in the Brugada Syndrome. *J Am Coll Cardiol*. 2015 Nov 3;66(18):1976-86.
6. Ohkubo K, Watanabe I, Okumura Y, et al. Right ventricular histological substrate and conduction delay in patients with Brugada syndrome. *Int Heart J* 2010;51:17–23.
7. Frustaci A, Priori SG, Pieroni M, et al. Cardiac histological substrate in patients with clinical phenotype of Brugada syndrome. *Circulation* 2005;112:3680–7.

8. Ten Sande JN, Coronel R, Conrath CE, Driessen AH, de Groot JR, Tan HL, Nademanee K, Wilde AA, de Bakker JM, van Dessel PF. ST-Segment Elevation and Fractionated Electrograms in Brugada Syndrome Patients Arise From the Same Structurally Abnormal Subepicardial RVOT Area but Have a Different Mechanism. *Circ Arrhythm Electrophysiol*. 2015 Dec;8(6):1382-92.
9. Matsuo K, Kurita T, Inagaki M, Kakishita M, Aihara N, Shimizu W, Taguchi A, Suyama K, Kamakura S, Shimomura K. The circadian pattern of the development of ventricular fibrillation in patients with Brugada syndrome. *Eur Heart J*. 1999;20(6):465-70.
10. Mizumaki K, Fujiki A, Tsuneda T, Sakabe M, Nishida K, Sugao M, Inoue H. Vagal activity modulates spontaneous augmentation of ST elevation in the daily life of patients with Brugada syndrome. *J Cardiovasc Electrophysiol*. 2004;15(6):667-73.
11. Papadatos GA, Wallerstein PM, Head CE, Ratcliff R, Brady PA, Benndorf K, Saumarez RC, Trezise AE, Huang CL, Vandenberg JI, Colledge WH, Grace AA. Slowed conduction and ventricular tachycardia after targeted disruption of the cardiac sodium channel gene *Scn5a*. *Proc Natl Acad Sci U S A*. 2002 Apr 30;99(9):6210-5.
12. Schilling RJ, Davies DW, Peters NS. Characteristics of sinus rhythm electrograms at sites of ablation of ventricular tachycardia relative to all other sites: a noncontact mapping study of the entire left ventricle. *J Cardiovasc Electrophysiol*. 1998; 9: 921-933.
13. Franz MR, Bargheer K, Rafflenbeul W, Haverich A, Lichtlen PR. Monophasic action potential mapping in human subjects with normal electrocardiograms: direct evidence for the genesis of the T wave. *Circulation*. 1987;75(2):379-86.
14. Yue AM, Paisey JR, Robinson S, Betts TR, Roberts PR, Morgan JM. Determination of human ventricular repolarization by noncontact mapping: validation with monophasic action potential recordings. *Circulation*. 2004 ;110(11):1343-50.

15. Potse M, Coronel R, Opthof T, Vinet A. The positive T wave. *Anadolu Kardiyol Derg.* 2007 Jul;7 Suppl 1:164-7.
16. Potse M, Vinet A, Opthof T, Coronel R. Validation of a simple model for the morphology of the T wave in unipolar electrograms. *Am J Physiol Heart Circ Physiol.* 2009;297(2):H792-801.
17. Taggart P, Sutton P, Chalabi Z, Boyett MR, Simon R, Elliott D, Gill JS. Effect of adrenergic stimulation on action potential duration restitution in humans. *Circulation.* 2003 ;107(2):285-9.
18. Hanson B, Sutton P, Elameri N, Gray M, Critchley H, Gill JS, Taggart P. Interaction of activation-repolarization coupling and restitution properties in humans. *Circ Arrhythm Electrophysiol.* 2009 Apr;2(2):162-70.
19. Kawara T, Derksen R, de Groot JR, Coronel R, Tasseron S, Linnenbank AC, Hauer RN, Kirkels H, Janse MJ, de Bakker JM. Activation delay after premature stimulation in chronically diseased human myocardium relates to the architecture of interstitial fibrosis. *Circulation.* 2001; **104**: 3069–3075
20. Coronel R, Casini S, Koopmann TT, Wilms-Schopman FJ, Verkerk AO, de Groot JR, Bhuiyan Z, Bezzina CR, Veldkamp MW, Linnenbank AC, van der Wal AC, Tan HL, Brugada P, Wilde AA, de Bakker JM. Right ventricular fibrosis and conduction delay in a patient with clinical signs of Brugada syndrome: a combined electrophysiological, genetic, histopathologic, and computational study. *Circulation.* 2005; 112: 2769–2777.
21. Opthof T, Remme CA, Jorge E, et al Cardiac activation-repolarization patterns and ion channel expression mapping in intact isolated normal human hearts. *Heart Rhythm.* 2017;14(2):265-272.

22. Meregalli PG, Wilde AA, Tan HL. Pathophysiological mechanisms of Brugada syndrome: depolarization disorder, repolarization disorder, or more? *Cardiovasc Res*. 2005 Aug 15;67(3):367-78. Review

23. Hoogendijk MG, Potse M, Linnenbank AC, Verkerk AO, den Ruijter HM, van Amersfoort SC, Klaver EC, Beekman L, Bezzina CR, Postema PG, Tan HL, Reimer AG, van der Wal AC, Ten Harkel AD, Dalingshaus M, Vinet A, Wilde AA, de Bakker JM, Coronel R. Mechanism of right precordial ST-segment elevation in structural heart disease: excitation failure by current-to-load mismatch. *Heart Rhythm*. 2010;7:238–248.

24. Hoogendijk MG, Potse M, Vinet A, de Bakker JM, Coronel R. ST segment elevation by current-to-load mismatch: an experimental and computational study. *Heart Rhythm*. 2011;8:111–118.

25. Nakazawa K, Sakurai T, Takagi A, Kishi R, Osada K, Nanke T, Miyake F, Matsumoto N, Kobayashi S. Autonomic imbalance as a property of symptomatic Brugada syndrome. *Circ J*. 2003;67(6):511-4.

26. Wichter T, Matheja P, Eckardt L, Kies P, Schäfers K, Schulze-Bahr E, Haverkamp W, Borggrefe M, Schober O, Breithardt G, Schäfers M. Cardiac autonomic dysfunction in Brugada syndrome. *Circulation*. 2002;105(6):702-6.

27. Yan GX, Antzelevitch C. Cellular basis for the Brugada syndrome and other mechanisms of arrhythmogenesis associated with ST-segment elevation. *Circulation* 1999;100:1660–6.

28. Leong KMW, Ng FS, Yao C, Roney C, Taraborrelli P, Linton NWF, Whinnett ZI, Lefroy DC, Davies DW, Boon Lim P, Harding SE, Peters NS, Kanagaratnam P, Varnava AM. ST-Elevation Magnitude Correlates With Right Ventricular Outflow Tract Conduction Delay in Type I Brugada ECG. *Circ Arrhythm Electrophysiol*. 2017;10(10). pii: e005107. doi: 10.1161/CIRCEP.117.005107.

29. Leong KMW, Ng FS, Roney C, Cantwell C, Shun-Shin MJ, Linton NWF, Whinnett ZI, Lefroy DC, Davies DW, Harding SE, Lim PB, Francis D, Peters NS, Varnava

AM, Kanagaratnam P. Repolarization abnormalities unmasked with exercise in sudden cardiac death survivors with structurally normal hearts. *J Cardiovasc Electrophysiol.* 2018;29(1):115-126. doi: 10.1111/jce.13375.

30. Nademanee K, Veerakul G, Chandanamattha P, Chaothawee L, Ariyachaipanich A, Jirasirojanakorn K, Likittanasombat K, Bhuripanyo K, Ngarmukos T. Prevention of ventricular fibrillation episodes in Brugada syndrome by catheter ablation over the anterior right ventricular outflow tract epicardium. *Circulation.* 2011;123(12):1270-9.

31. Pappone C, Brugada J, Vicedomini G, Ciconte G, Manguso F, Saviano M, Vitale R, Cuko A, Giannelli L, Calovic Z, Conti M, Pozzi P, Natalizia A, Crisà S, Borrelli V, Brugada R, Sarquella-Brugada G, Guazzi M, Frigiola A, Menicanti L, Santinelli V. Electrical Substrate Elimination in 135 Consecutive Patients With Brugada Syndrome. *Circ Arrhythm Electrophysiol.* 2017;10(5):e005053.

Figure Legends

Figure 1. Positioning of Mapping Catheters in the RV and great cardiac vein to record RV endocardial and epicardial electrograms.

Figure 2 . Endo and Epicardial Activation time dynamics pre and post edrophonium in control and Brugada hearts.

Figure 3. Endo and Epicardial ARI dynamics pre and post edrophonium in control and Brugada Hearts.

Figure 4. Example of Sinus rhythm ECG and Electrograms Recorded epi and endocardially in a Control and BrS patient. There is a type II coved ST elevation pattern resting ECG of the BrS patient which is reflected in the epicardial unipolar electrograms- these are exaggerated after edrophonium (blue) as well as a decrease in activation times

in the epicardial electrograms . No significant change occurs in the control after the edrophonium.

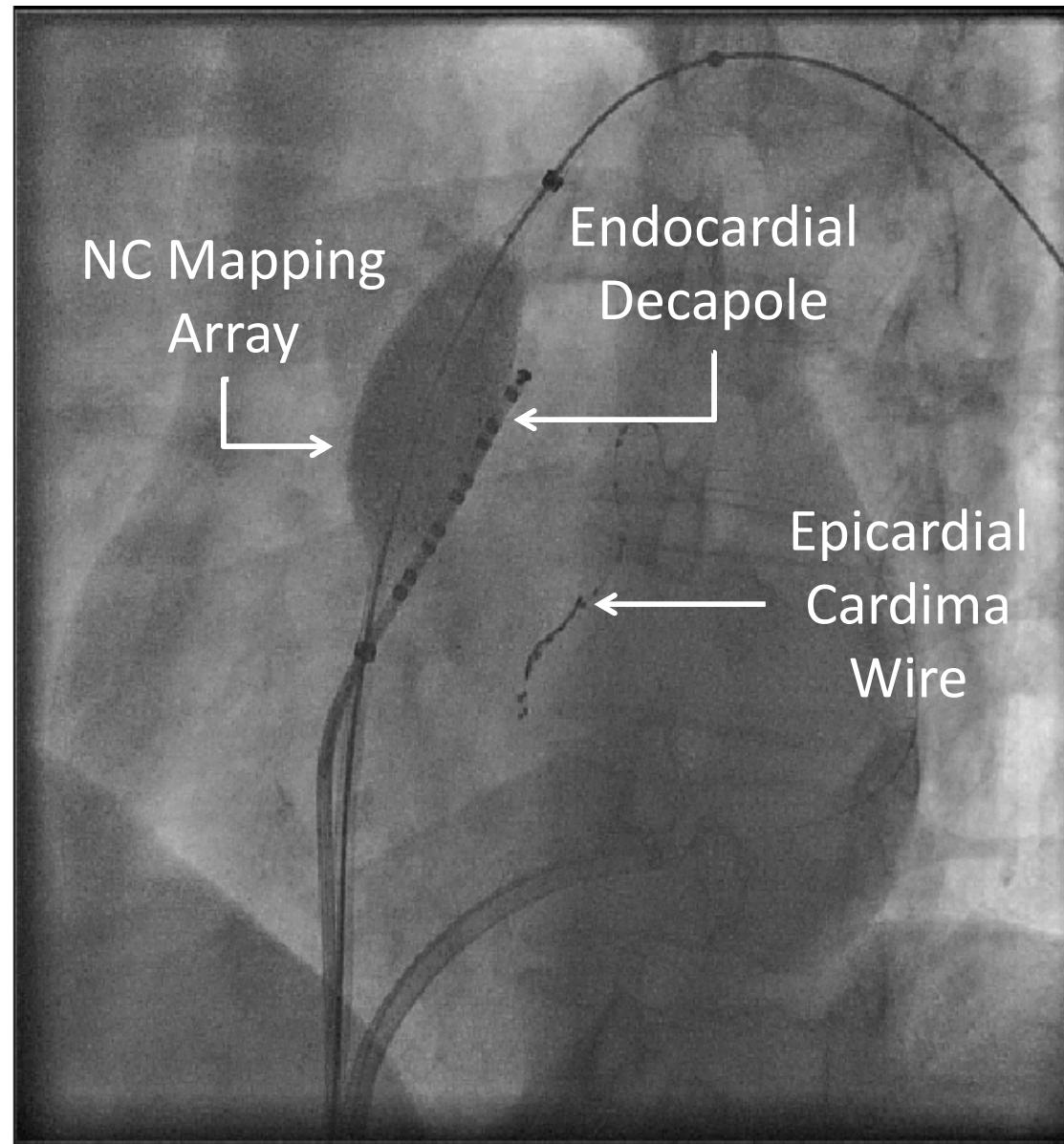
Figure 5. Endo and Epicardial Repolarisation Time dynamics pre and post edrophonium in control and Brugada Hearts.

Supplemental Figure S1 . Example of semi-automated AT, ARI and RT measurements from intracardiac Non-contact unipolar signals. The blue interrupted line is the dV/dt of the solid black line (which is the signal exported from Ensite NC mapping system). The red coloured squares mark activation times (dV/dt min) and the blue dV/dt max of the T wave upstroke to measure ARI: the Wyatt method was used to look at all T waves employing upstroke of the T wave.

Supplemental Figure S2. A. Baseline Epicardial AT, ARI and RT in Controls and BrS during steady state pacing at 400ms. *P<0.05 between control and BrS. **B.** Baseline Endocardial AT, ARI and RT in Controls and BrS during steady state pacing at 400ms. *P<0.05 between control and BrS.

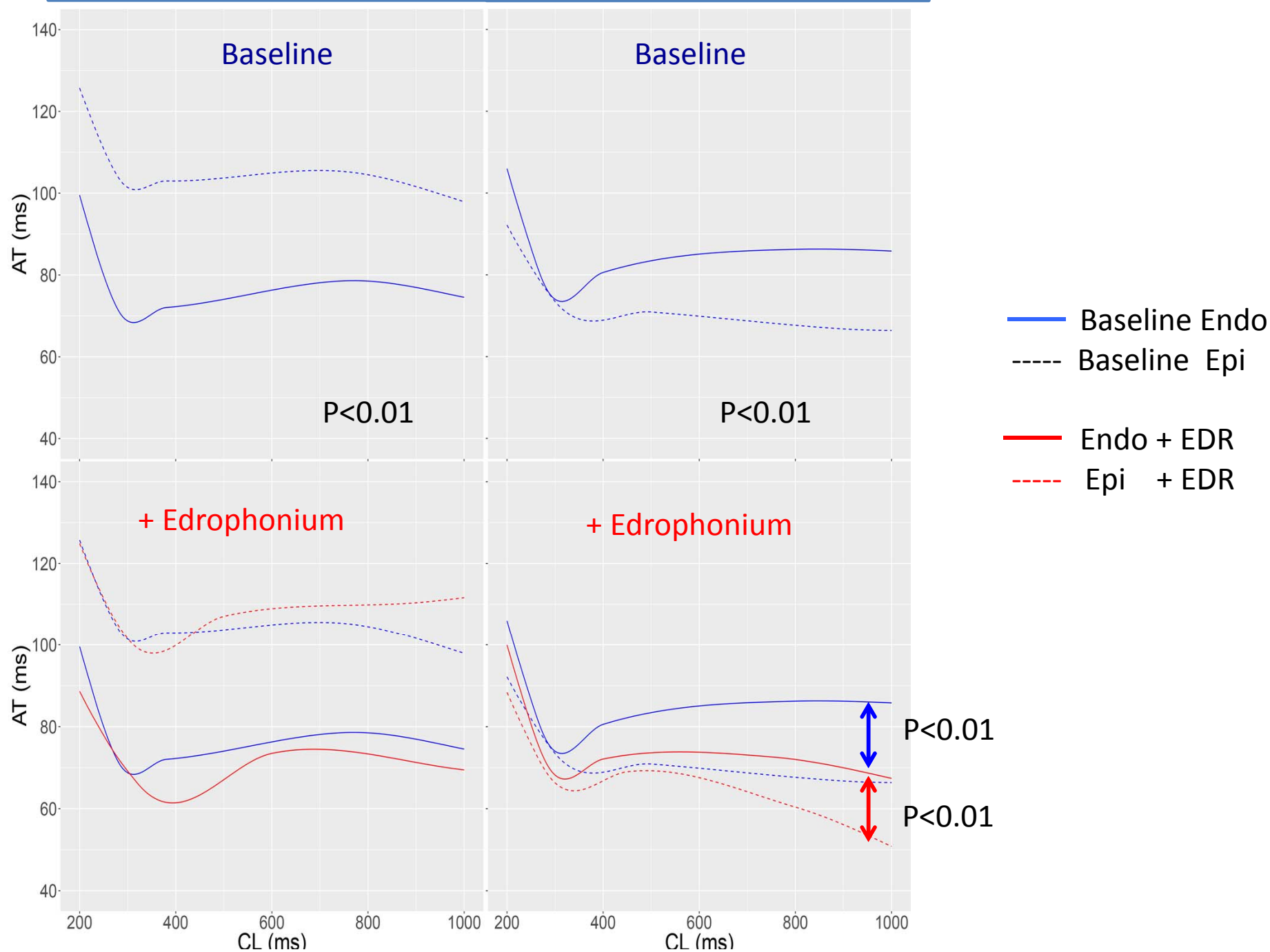
Supplemental Figure S3

Boxplots representing the mean increase delay (MID), endocardially (Endo) and epicardially (Epi), for both Control and Brugada subjects, before (Base) and after Edrophonium (Edr) administration. For the control group, a significant difference in the MID between endocardial and epicardial regions was induced by drug administration. For the Brugada group, a significant difference was already present at baseline and was further exacerbated. These difference were mainly due to a MID prolongation in the epicardium. *P<0.05 **P<0.01 ***P<0.001



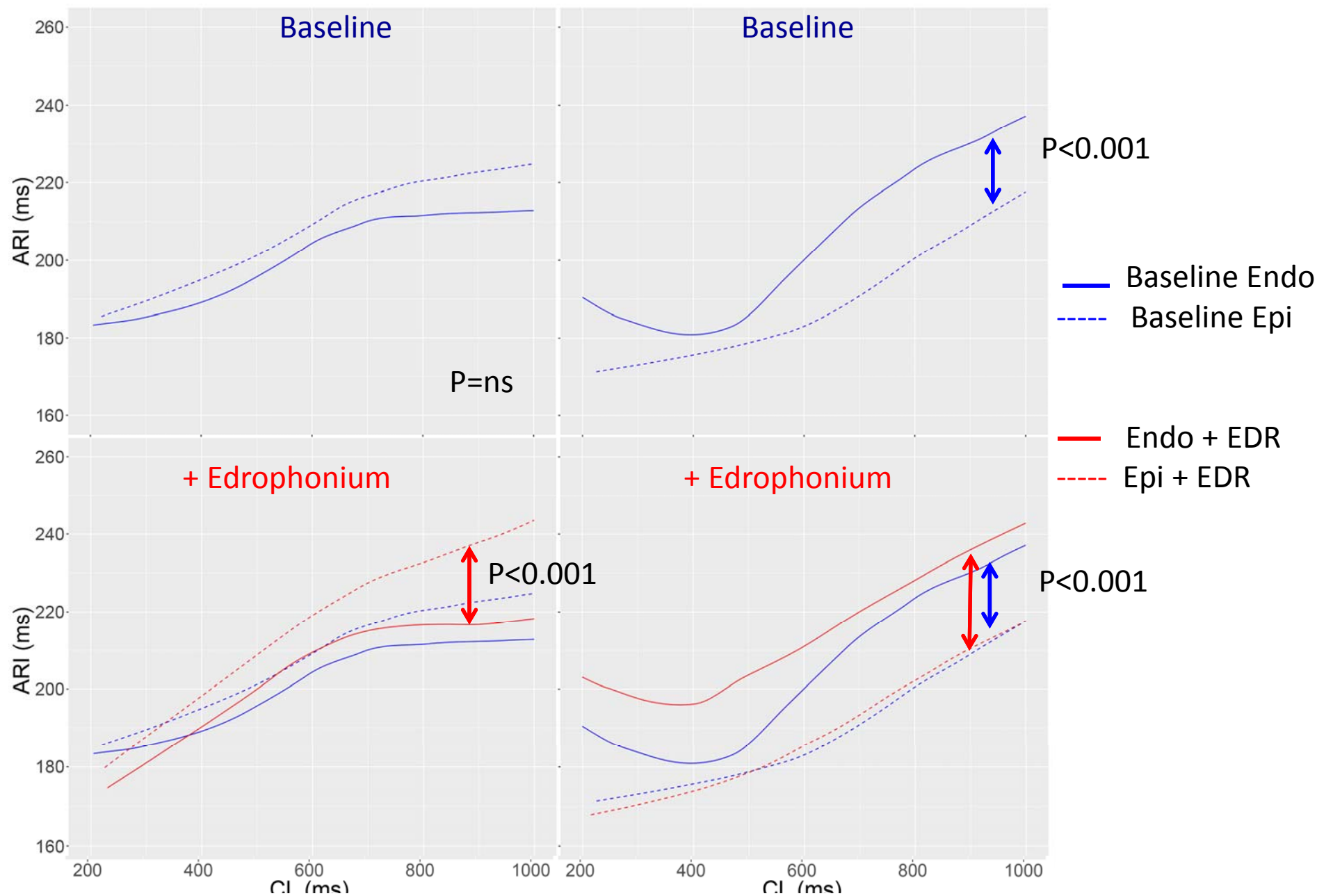
Activation Time Control

Activation Time Brugada

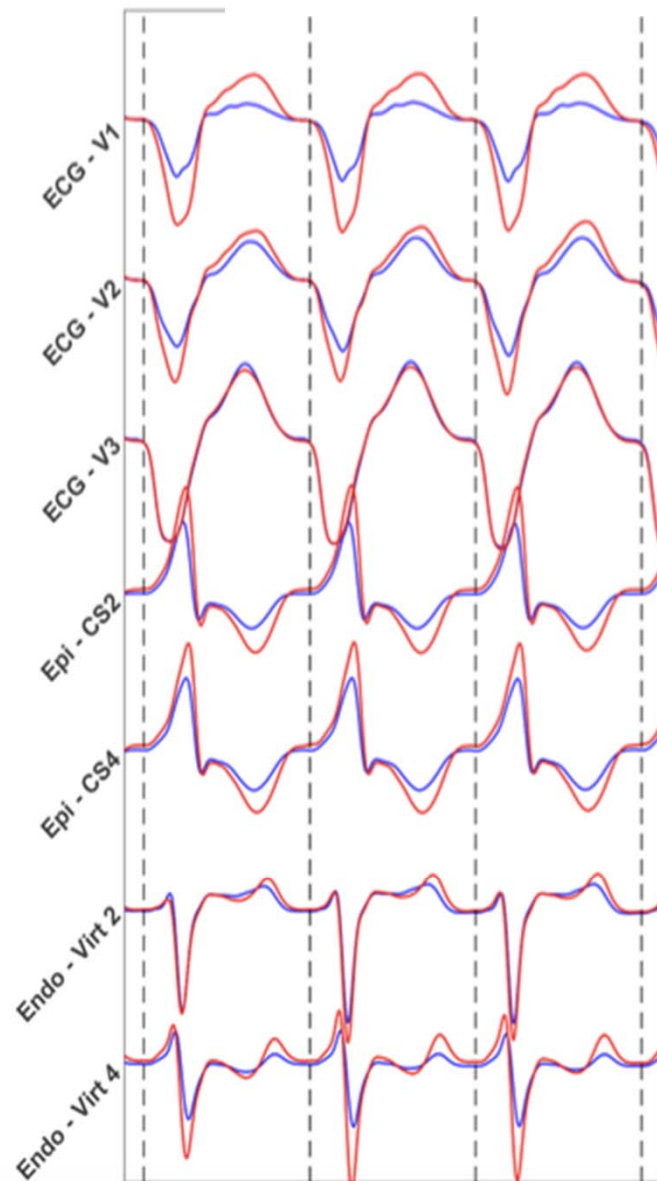


Activation Recovery Interval Control

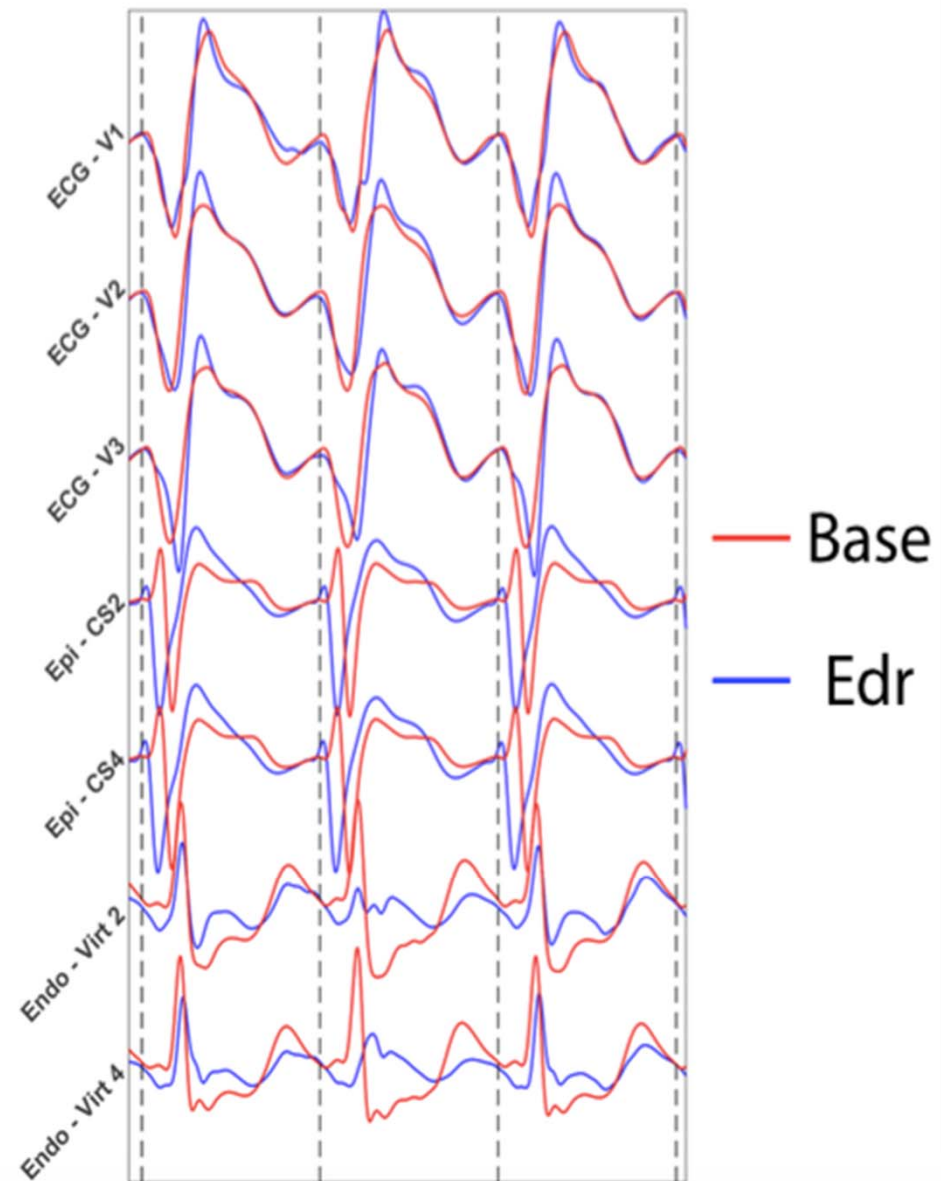
Activation Recovery Interval Brugada



Control



BrS



Repolarization Time Control

Repolarization Time Brugada

